Cation Diffusion in $MGaBr_4$ (M = Li, Cu, and Ag) Studied by ^7Li, ^{63}Cu, and ^{71}Ga NMR, ^{81}Br NQR, and Conductivity

Yasumasa Tomita, Koji Yamada,* Hiroshi Ohki, and Tsutomu Okuda

Department of Chemistry, Faculty of Science, Hiroshima University, Kagamiyama 1-3-1, Higashi-Hiroshima 739

(Received April 28, 1997)

Cation diffusion in $MGaBr_4$ (M = Li, Cu) was confirmed by measuring the temperature dependence of the ^7Li and ^{63}Cu NMR linewidths. The activation energies for the cation diffusion were determined to be 36 and 44 kJ mol^{-1} for $LiGaBr_4$ and $CuGaBr_4$, respectively. The activation energy for the reorientation of the $GaBr_4^-$ anion in $CuGaBr_4$ was evaluated to be 62 kJ mol^{-1} from ^{71}Ga NMR. The cation diffusion was also confirmed for $MGaBr_4$ (M = Cu, Ag) by observing a modulation effect on the ^{81}Br NQR T_1. As expected from the modulation effect of NQR, the ionic conductivity of $AgGaBr_4$ was one order higher than that of $CuGaBr_4$.

In our previous papers we reported on the motional narrowing of the ^7Li and ^{63}Cu NMR lines due to cation diffusion, and discussed the effects of cation diffusion and reorientation of the AlX_4^- (X = Cl, Br) anion based on the results of halogen NQR.[1,2] The correlation times (τ_c) and activation energies (E_a) for the motions were also determined from these experiments. In general, from a measurement of the NMR linewidth on a quadrupolar nucleus, the onset of cation diffusion could not be detected using a powdered sample because of broadening due to the quadrupole effect. Although a time-averaged quadrupole splitting over the motion may provide useful information concerning the mechanism of the diffusion, quantitative parameters, such as E_a and τ_c, are estimated more directly from a linewidth measurement using a single crystal or from a relaxation measurement.[3—5]

In our previous measurements, single crystals were used to avoid broadening due to the quadrupole interaction and the chemical-shift anisotropy.[1,2] In a favorable case, such as $LiAlBr_4$ or $CuAlBr_4$, cation diffusion was also detected as a modulation effect on the NQR T_1. Although this effect has been reported for many compounds containing reorientationable groups near to the probe nucleus,[6—9] only a few examples have been reported concerning diffusion of the counter ion.[1,2] This technique is especially favorable if the movable probe nucleus has no magnetic moment, or low sensitivity, like Ag.

In this study we evaluated the rates and activation energies for the diffusional processes by means of ^7Li and ^{63}Cu NMR using single crystals. The effect of cation diffusion on the spin-lattice relaxation times of ^{81}Br NQR was also examined. The ionic conductivity of $MGaBr_4$ (M = Li, Cu, and Ag) is discussed on the basis of the NMR and NQR parameters and compared with previous studies.

Experimental

A single crystal of $MGaBr_4$ was grown form a melt containing stoichiometric amounts of MBr and $GaBr_3$ by a Bridgman technique. Samples were identified by a powder X-ray diffractometer (Rigaku Rad-B system) using Cu $K\alpha$ radiation. A home-built attachment was used to protect these hygroscopic samples from moisture.

^7Li, ^{63}Cu, and ^{71}Ga NMR were observed using a Matec pulsed spectrometer at 6.37 T with the corresponding Larmor frequencies of 105.41, 71.89, and 82.71 MHz, respectively. A similar Matec pulsed spectrometer was also used to detect ^{81}Br NQR, and its spin-lattice relaxation time was determined by a conventional pulse technique. The electric conductivity was determined by means of a complex impedance method at 10 different frequencies (100 Hz—100 kHz, ANDO LCR meter AG-4311B).

Results and Discussion

Structure and ^{63}Cu NMR Spectra for $CuGaBr_4$. The powder X-ray diffraction of $CuGaBr_4$ revealed that it belongs to a tetragonal system (space group: $P\bar{4}2c$) with $a = 5.706$ and $c = 10.638$ Å and is isomorphous with $CuGaCl_4$.[10] The Cu^+ cation is tetrahedrally coordinated by four Br atoms and its site symmetry is $\bar{4}$, as shown in Fig. 1. This is in marked contrast to $LiGaBr_4$ and $AgGaBr_4$, in which the cation is surrounded octahedrally by six Br atoms. The structure of $CuGaCl_4$ suggests that both the quadrupole and chemical-shift tensors are cylindrical ($\eta = 0$) about the axis parallel to the tetragonal c-axis.

Figure 2 shows the ^{63}Cu NMR spectrum observed for a powdered sample. The spectrum is governed mainly by a first-order quadrupole interaction, since the satellite transitions ($m = \pm 3/2 \Leftrightarrow \pm 1/2$) are symmetrical about the central transition ($m = -1/2 \Leftrightarrow 1/2$). Although two pairs of shoulders, which are characteristic of the first-order quadrupole interaction, are expected for the quadrupolar nucleus with $I = 3/2$, only the inner pair could be detected, as shown in Fig. 2. The quadrupole coupling constant (e^2Qq/h) at the Cu site was calculated from the frequency separation between a pair of inner shoulders ($\Delta\nu$) as

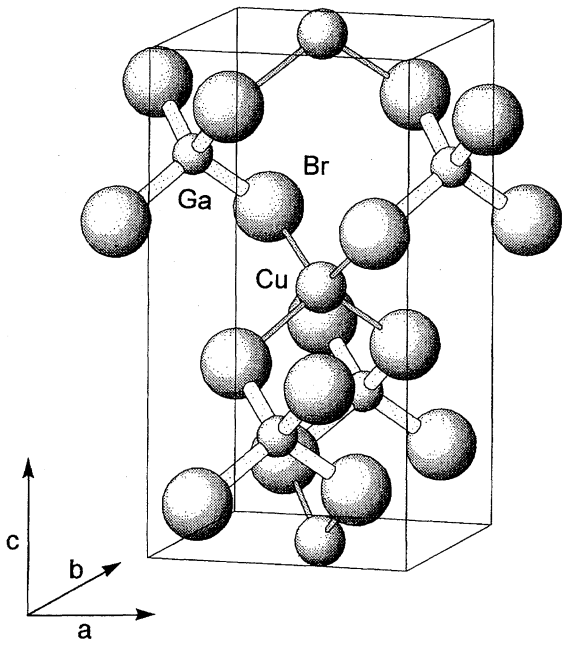

Fig. 1. Crystal structure of tetragonal $CuGaBr_4$.

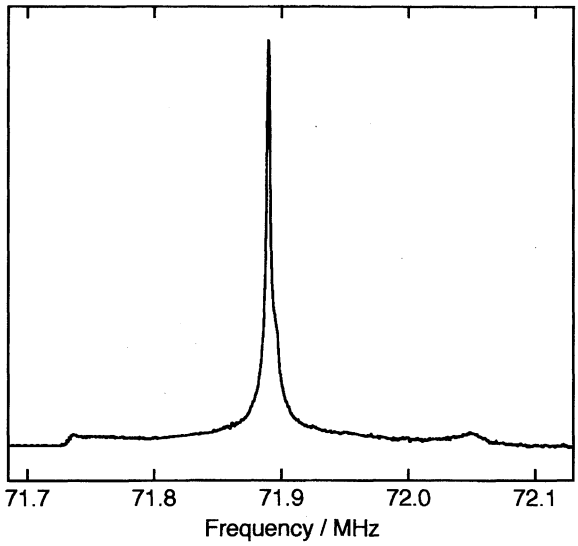

Fig. 2. ^{63}Cu NMR spectra for powdered $CuGaBr_4$ at 283 K.

$$e^2Qq/h = 2\cdot\Delta\nu. \quad (1)$$

The quadrupole coupling constant was evaluated to be 630 kHz from this equation. On the other hand, the central transition was asymmetrical, and its linewidth was ca. 10 kHz, as shown in Fig. 2. The second-order quadrupole effect on this transition was estimated to be only 0.7 kHz from the e^2Qq/h stated above. The linewidth due to the dipole–dipole interaction was 2.14 kHz based on a measurement using a single crystal, as described below. This finding suggests that the central transition of ^{63}Cu NMR in $CuGaBr_4$ is a convolution of the chemical-shift anisotropy and the dipole–dipole interactions. Figure 3 shows the observed spectra of the central transition at 289 and 495 K together with the results of simulations. Table 1 summarizes the parameters used

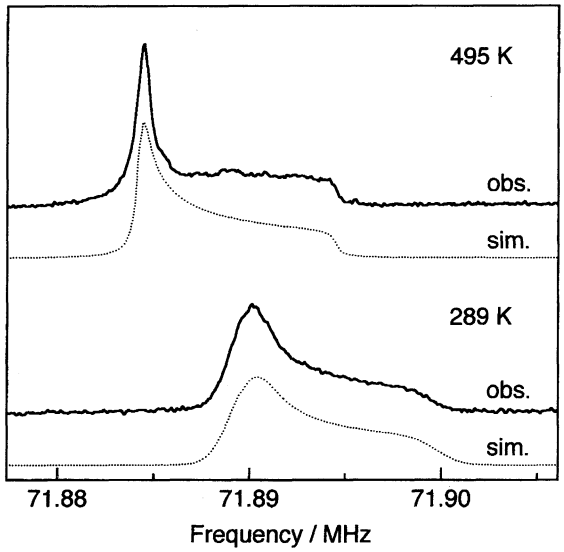

Fig. 3. Temperature dependence of the ^{63}Cu NMR central transition for $CuGaBr_4$ using a powdered sample. Solid lines are observed spectra and dotted lines are simulated spectra.

Table 1. NMR Parameters of ^{63}Cu for $CuGaBr_4$

		285 K	495 K
e^2Qqh^{-1}/kHz		630	—
Chemical shift anisotropy[a]/ppm	$\sigma_{\parallel}$	−47	−121
	$\sigma_{\perp}$	94	20
	σ_{iso}	0	−74
Dipole–dipole interaction/kHz		2.1	0.3

a) Relative to crystalline CuBr.

in these simulations for $CuGaBr_4$. It is interesting to note that the chemical-shift anisotropy remains at 495 K, but the dipole–dipole interaction is averaged out.

Motional Narrowing of ^7Li, ^{63}Cu, and ^{71}Ga NMR Using Single Crystals. Figures 4 and 5 plot the linewidths of the ^7Li, ^{63}Cu, and ^{71}Ga NMR spectra against the temperatures. These measurements were carried out on the central transitions ($m=-1/2\Leftrightarrow 1/2$) using single crystals. With increasing temperature, the motional narrowings of ^7Li and ^{63}Cu spectra began at about 260 and 320 K, respectively. The linewidth narrowed from 4.5 to 0.5 kHz for ^7Li and from 2.2 to 0.3 kHz for ^{63}Cu NMR. The narrowing behavior and the linewidth at the narrowing limit suggest the presence of the translational diffusion of cations. The linewidth transition of ^{71}Ga NMR was also observed for $CuGaBr_4$ above 400 K due to the reorientation of the $GaBr_4^-$ anion, although the motional narrowing was not so drastic as that found in the ^{63}Cu NMR spectra. The correlation times (τ_c) for these motions were evaluated by the following equation:[11]

$$\tau_c = (1/\alpha\delta\omega)\tan[\pi(\delta\omega^2 - \delta\omega_A^2)/2(\delta\omega_B^2 - \delta\omega_A^2)], \quad (2)$$

where $\delta\omega_A$, $\delta\omega$, and $\delta\omega_B$ are the linewidths above, within, and below the transition region, respectively; α is a numerical constant of approximately unity. Figure 6 shows

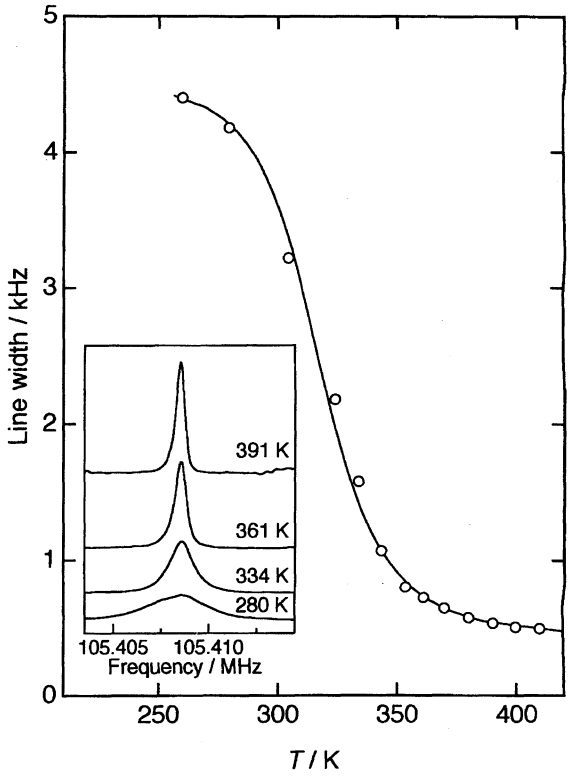

Fig. 4. Temperature dependence of ^{7}Li NMR linewidth as a function of temperature. The linewidth of the $m=-1/2\Leftrightarrow 1/2$ transition was observed using a single crystal.

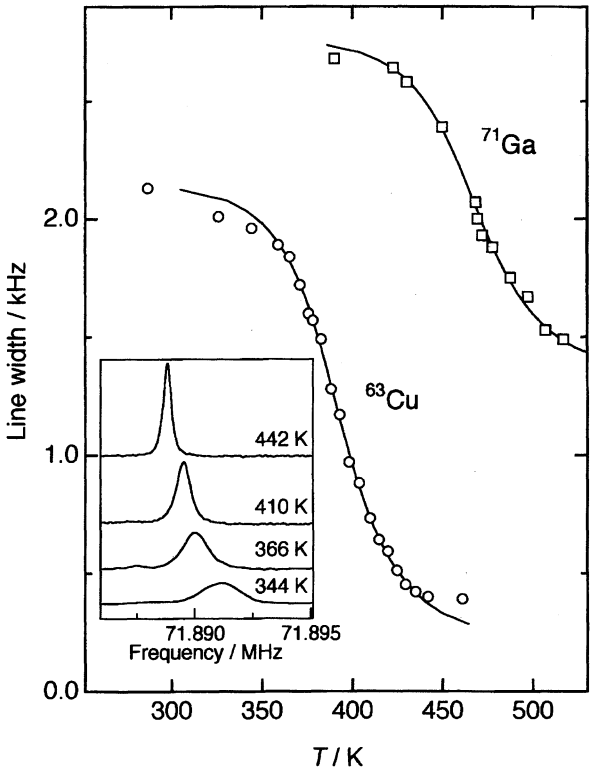

Fig. 5. Temperature dependence of ^{63}Cu and ^{71}Ga NMR linewidths as a function of temperatures. The linewidths of the $m=-1/2\Leftrightarrow 1/2$ transitions were observed using a single crystal.

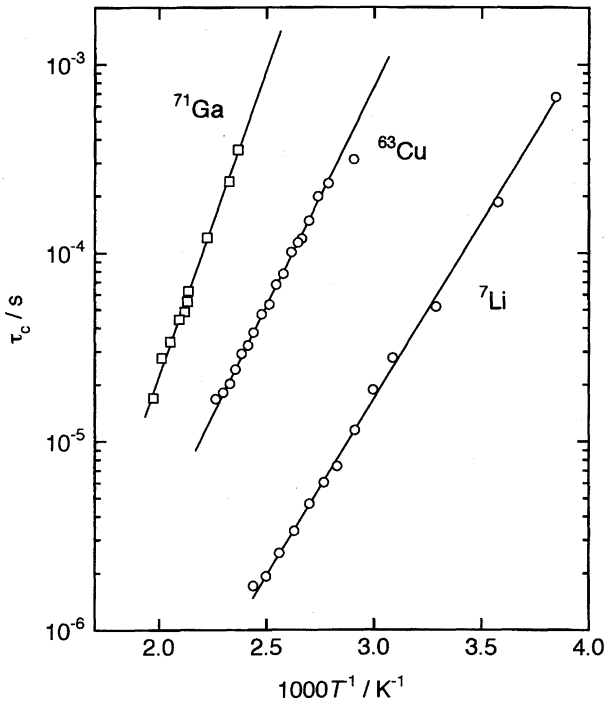

Fig. 6. Temperature dependence of the correlation times for $MGaBr_4$ (M=Li and Cu).

plots of the correlation time against the inverse temperature. τ_c as well as $\delta\omega_A$ and $\delta\omega_B$ were evaluated from fitting the observed linewidth to Eq. 2 by the use of a non-linear least-squares method. The values of $\delta\omega_A$ and $\delta\omega_B$ are 2.14 and 0.20 kHz for ^{63}Cu NMR and 2.76 and 1.32 kHz for ^{71}Ga NMR in $CuGaBr_4$. The straight line in Fig. 6 was drawn assuming an Arrhenius equation,

$$\tau_c = \tau_0 \exp(E_a/RT), \tag{3}$$

where E_a is the activation energy for the diffusion or reorientational motion and τ_0 is the pre-exponential parameter. These parameters are summarized in Table 2.

^{81}Br NQR of $MGaBr_4$ (M=Li, Cu, and Ag). Table 3 lists of the NQR frequencies for these three compounds. The temperature dependence of the ^{81}Br NQR frequencies for $MGaBr_4$ (M=Cu, Ag) are given in Fig. 7. Four ^{81}Br NQR signals were observed from 77 K to the melting point for both $LiGaBr_4$ and $AgGaBr_4$. As expected from the crystal structure, only one ^{81}Br NQR signal was observed for $CuGaBr_4$. With increasing temperature, the ^{81}Br NQR frequencies for all three compounds decreased continuously and showed no indication of a phase transition. Figure 8 shows the temperature dependence of the spin-lattice relaxation times, suggesting the dynamic aspects of these compounds. T_1 of all signals gradually decreased with increasing temperature up to ca. 300 K, and then decreased exponentially. The relaxation rate (T_1^{-1}), can be expressed as[12,13]

$$(T_1^{-1})_{obs} = (T_1^{-1})_{Raman} + (T_1^{-1})_{reor} + (T_1^{-1})_{mod}, \tag{4a}$$

where

$$(T_1^{-1})_{Raman} = aT^n, \tag{4b}$$

Table 2. Dynamic Properties of $MGaBr_4$ (M = Li, Cu, and Ag)

Compound	Method	E_a/kJ mol^{-1}	τ_0/s or b^{-1}/s	Motional mode for E_a
$LiGaBr_4$	^{81}Br NQR	52	1.4×10^{-10}	
	^{7}Li NMR	36	9.3×10^{-11}	Li^+ diffusion
$CuGaBr_4$	^{81}Br NQR	48	3.2×10^{-10}	Cu^+ diffusion
	^{63}Cu NMR	44	1.9×10^{-10}	Cu^+ diffusion
	^{71}Ga NMR	62	1.7×10^{-11}	$GaBr_4^-$ reorientation
	Conductivity	49		
$AgGaBr_4$	^{81}Br NQR	32	7.0×10^{-9}	Ag^+ diffusion
	Conductivity	51		

Table 3. NQR Frequencies for $MGaBr_4$ (M = Li, Cu, and Ag)

Compound	Nucleus	Frequency/MHz	
		77 K	297 K
$CuGaBr_4$	^{81}Br	111.199	109.575
$LiGaBr_4$	^{81}Br	99.407	98.968
		102.696	101.191
		115.459	113.156
		123.277	120.204
$AgGaBr_4$	^{81}Br	95.172	94.175
		100.435	99.994
		110.354	107.444
		118.092	113.654

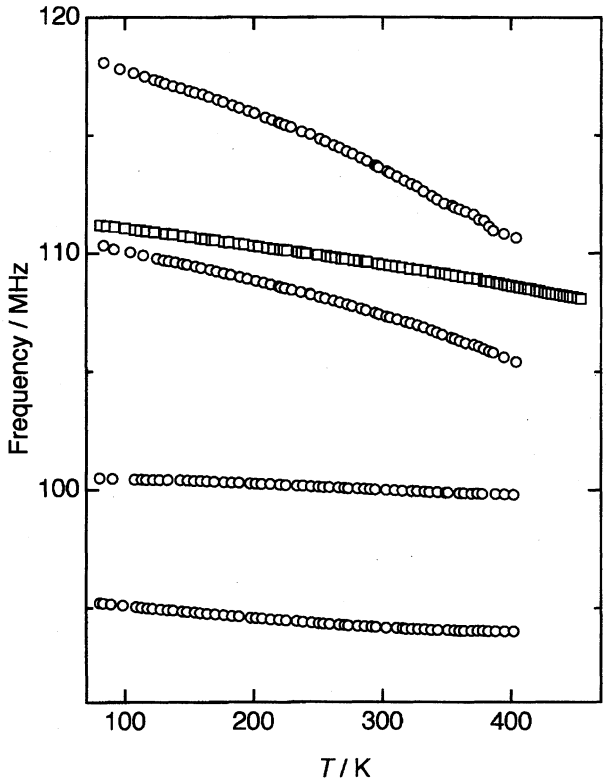

Fig. 7. Temperature dependence of ^{81}Br NQR frequencies for $MGaBr_4$ (M = Cu: marked by squares and Ag: marked by circles).

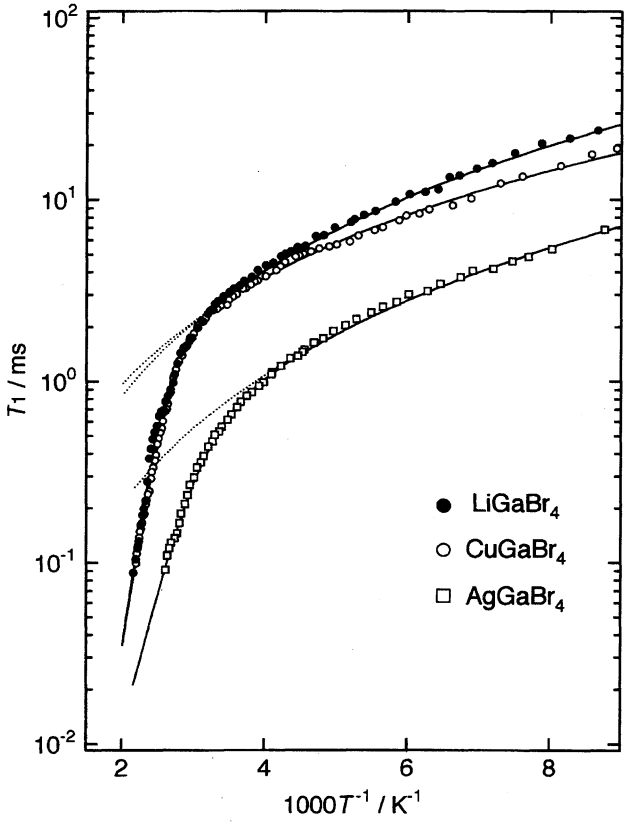

Fig. 8. Temperature dependence of ^{81}Br NQR T_1 for $MGaBr_4$. Solid lines are best-fit curves assuming Eq. 4a.

$$(T_1^{-1})_{reor} = b\exp(E_a/RT). \quad (4c)$$

The first term in Eq. 4a represents the contribution from the Raman process (n=2) which governs the behavior at low temperature; the second term represents the contribution from a reorientation of the fragment containing the monitored nucleus. The third contribution, which is called the modulation effect, arises from the EFG fluctuation due to nearby fragments, and is expressed as

$$(T_1^{-1})_{mod} = b'\exp(E_a'/RT), \quad (4d)$$

with

$$b' = (2/3)(q'/q)^2\tau_0^{-1},$$

where q'/q is a fractional part of the fluctuating EFG. In these compounds there are two possible contributions to the

activation process: the reorientation of the $GaBr_4^-$ anion expressed as $(T_1^{-1})_{reor}$, and the diffusion of the cation, expressed as $(T_1^{-1})_{mod}$. If these two activation processes contribute simultaneously, the experimentally obtained activation energy corresponds to a process having a larger E_a. In the case of $CuGaBr_4$, the activation energy was estimated to be 48 kJ mol^{-1}, which is consistent with that of Cu diffusion from the ^{63}Cu NMR experiment, and is lower than that of the reorientation of the $GaBr_4^-$ anion based on the ^{71}Ga NMR experiment. This suggests that the activation process detected in the ^{81}Br NQR T_1 can be assigned to a modulation effect due to cation diffusion. A similar modulation effect was observed for $AgGaBr_4$, for which E_a was estimated to be 32 kJ mol^{-1}. The onset of the Ag^+ diffusion could be indirectly confirmed by an NQR measurement, although Ag NMR could not be detected by our spectrometer. These NQR parameters are summarized in Table 2 together with the NMR parameters.

Ionic Conductivity of $MGaBr_4$ and the Mechanism. From the diffusional E_a values determined by NMR and NQR observations, the ionic conductivities were expected to increase in the order Cu<Li<Ag salt. The conductivity for $AgGaBr_4$ was higher than that of $CuGaBr_4$, as expected. The conductivity for $LiGaBr_4$ could not be determined because of its strong hygroscopic property. Figure 9 plots the conductivity (σ) against inverse temperature. The activation energy for the conduction was determined by the following equation:[14]

$$\sigma T = A \exp(-E_a/RT). \quad (5)$$

Table 2 summarizes E_a evaluated from Eq. 5. The E_a value for $CuGaBr_4$ is consistent with those derived from ^{63}Cu NMR and ^{81}Br NQR. However, the value of $AgGaBr_4$ is much higher than that from ^{81}Br NQR. It is uncertain whether this discrepancy arises from the local motional behavior of the cation or the difficulty to obtain a suitable sample for the conductivity measurement.

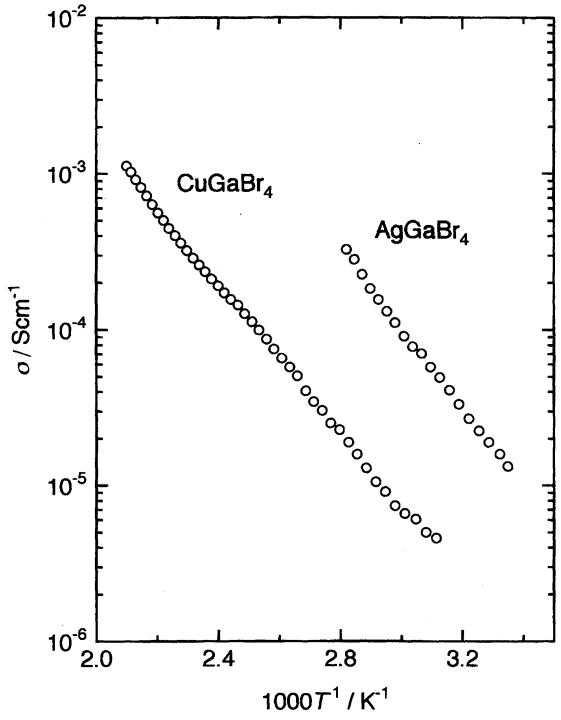

Fig. 9. Temperature dependence of the conductivity for $MGaBr_4$ (M = Cu and Ag).

According to Chandra,[15] these compounds can be classified into a category of a super-ionic solid having a molten sublattice type, because there is an excess of available tetrahedral and octahedral sites. As Fig. 3 shows, however, the broadening of the ^{63}Cu NMR spectra due to chemical-shift anisotropy did not change at all; nevertheless, the rate of the Cu^+ diffusion was fast enough to average out the chemical-shift anisotropy. This suggests that the Cu^+ ions jump between the tetrahedral sites, including interstitial sites, rather than the octahedral sites, in spite of its smaller free space for the cation; also, the directions of the principal axis of those tetrahedral sites are identical. This is due to the weak covalent bond which formed between the Cu and Br atoms using the sp^3 hybrid orbitals of Cu(I). The E_a values determined by the NMR narrowing process tend to decrease along with increasing the anionic radius for a series of $LiMX_4$ (M = Al and Ga). However, this feature could not be seen for $CuMX_4$ (M=Al and Ga) in which Cu^+ occupies a tetrahedral site.[16]

This work was supported by a Grant-in-Aid for Scientific Research on Priority Areas (No. 260) from the Ministry of Education, Science, Sports and Culture.

References

1) K. Yamada, M. Kinoshita, K. Hosokawa, and T. Okuda, *Bull. Chem. Soc. Jpn.*, **66**, 1317 (1993).
2) K. Yamada, Y. Tomita, and T. Okuda, *J. Mol. Struct.*, **34**, 5219 (1995).
3) K. Differt and R. Messer, *J. Phys. C*, **13**, 717 (1980).
4) R. Messer, H. Birli, and K. Differt, *J. Phys. C*, **14**, 2731 (1981).
5) D. Brinkmann, W. Freudenreich, and J. Roos, *Solid State Commun.*, **28**, 233 (1978).
6) D. E. Woessner and H. S Gutowsky, *J. Chem. Phys.*, **39**, 440 (1963).
7) J. A. S. Smith, "Advances in Nuclear Quadrupole Resonance," ed by J. A. S. Smith, Heyden, London (1974), Vol. 1, p. 115.
8) T. Okuda, K. Inui, A. Nakata, M. Katada, H. Terao, and K. Yamada, *J. Mol. Struct.*, **296**, 103 (1993).
9) Y. Tai, T. Asaji, D. Nakamura, and R. Ikeda, *Z. Naturforsch., Teil A*, **45A**, 477 (1990).
10) W. Honle, *Z. Kristallogr.*, **191**, 141 (1990).
11) A. Abragam, "Principles of Nuclear Magnetism," Oxford University Press, Oxford (1961), p. 455.
12) H. Chihara and N. Nakamura, "Advances in Nuclear Quadrupole Resonance," ed by J. A. S. Smith, Heyden, London (1980), Vol. 4, p. 1.
13) K. Yamada, K. Isobe, T. Okuda, and Y. Furukawa, *Z. Naturforsch., Teil A*, **49A**, 258 (1994).
14) Ph. Colomban and A. Novak, *J. Mol. Struct.*, **177**, 277 (1988).

15) S. Chandra, "Superionic Solid, Principles and Applications," North-Holland Publishing Company, Amsterdam (1981), p. 17.

16) W. Honle and A. Simon, *Z. Naturforsch.*, *Teil A*, **45A**, 1391 (1986).